ELSEVIER

Mechanisms of Development 53 (1995) 3–13

Analysis of the genes involved in organizing the tail segments of the *Drosophila melanogaster* embryo

D.T. Kuhn[a,*], G. Turenchalk[a], J.A. Mack[a], G. Packert[a], T.B. Kornberg[b]

[a]*Department of Biology, University of Central Florida, Orlando, FL 32816, USA*
[b]*Department of Biochemistry and Biophysics, University of California, San Francisco, CA 94143, USA*

Received 10 February 1995; revision received 10 April 1995; accepted 13 April 1995

Abstract

The metameric organization of the *Drosophila melanogaster* tail is obscured by developmental events that partially suppress or fuse some of its regions. To better define the developmental origins and segmental identities in the tail of the *Drosophila* embryo, we documented expression patterns and mutant phenotypes of several genes that play important roles in its morphogenesis. We documented the domains of *engrailed* (en), *Abdominal-B* (*Abd-B*) and *caudal* (*cad*) expression in the tail region. The staining pattern of *cut* (*ct*) was used to correlate the embryonic sense organs with their respective positions on the larval cuticle. The *en* patterns in different Bithorax-Complex (BX-C) *Abd-B* morphogenetic (*m*) and regulatory (*r*) mutants demonstrated that *Abd-B* functions to, among other things, suppress embryonic ventral epidermal structures on the posterior side of A8 to A9. Ventral epidermal structures were not added back into the *en* pattern in r^- or BX-C^- mutants, indicating that although the BX-C functions extend through A10, other non-BX-C genes must be required for development of this segment.

Keywords: Drosophila embryonic development; Tail segments; Homeotic genes

1. Introduction

Insects are comprised of metameres that are aligned in a repetitive arrangement along the anterior/posterior axis. In some regions, such as the thorax and the anterior abdomen, regular spacing, well-delineated boundaries, and distinctive features clearly distinguish the number and identity of segments. However, the precise organization of the head and tail is obscured by more complex arrangements of the constituent parts. Indeed, despite much effort and analysis, the segmental identity of some of the structures and, remarkably, the number of segments in these regions is unresolved. Morphological comparisons between different insect groups have provided important clues, as have more recent molecular and genetic studies of *Drosophila*.

Genetic and molecular studies have revealed how the set of maternal-effect, gap, pair-rule, and segment polarity genes pattern most of the *Drosophila* embryo (reviewed by St. Johnston and Nüsslein-Volhard, 1992). The concerted action of these genes subdivides the embryo into metameres, and the repetitive use of the same combinations of some of the genes throughout most of the embryo underscores the fundamental similarity between the metameres. In the thorax and in much of the head and abdomen, these genes function to place bands of *wingless* (*wg*) and *engrailed* (*en*) expression at either side of each parasegmental boundary. At the anterior and posterior tips, however, these roles do not persist, and the geometrically simple relationships between their domains of expression either do not form or they become obscured by complex morphogenetic movements. Even in *Drosophila*, the complexity of its developmental program has continued to frustrate efforts to understand the organization of its terminal regions.

Examples of the increased complexity in the tail region include the segment polarity genes *gooseberry-P* (*gsb-P*) and *gooseberry* (*gsb-D*) (Bopp et al., 1986; Gutjahr et al., 1993). Within each trunk segment, these genes are expressed in bands that coincide precisely with *wg*-expressing cells and overlap partially with *en*-expressing

* Corresponding author. Tel.: +1 407 8232976; Fax: +1 407 8235769; E-mail: fdkuhn@ucf1vm.bitnet.

0925-4773/95/$09.50
SSDI 0925-4773(95)00399-L

cells (Gutjahr et al., 1993). The importance of these patterns of expression is revealed in *gsb* mutants, in which *wg* transcripts in the ventral regions at stage 11 disappear, and in *wg* mutants in which *gsb-D* transcripts in the trunk disappear (Baumgartner et al., 1987; Hidalao, 1991). In the embryonic tail, an additional *gsb* band forms in a region with no *wg* or *en* expression (Baumgartner et al., 1987). This *gsb* band is independent of *wg* function.

In addition to the set of segmentation genes that delineate the metameres, a unique combination of homeotic genes function to establish an identity for each parasegment (see reviews by McGinnis and Krumlauf, 1992; Lawrence and Morata, 1994). Genes of the Antennapedia Complex function in the head and anterior thorax, while the genes of the BX-C function from posterior thoracic segment 1 (pT1) at least through abdominal segment 9 (PS4–PS14; Lewis 1978; Casanova et al., 1986). Of the three homeotic genes in the BX-C (*Ubx*, *abd-A* and *Ab-B*), the *Abd-B* gene provides identity to the posterior abdomen. *Abd-B* has been subdivided into proximal morphogenetic (*m*) and distal regulatory (*r*) functions (Casanova et al., 1986). The *m* function is encoded by the class A transcript which is present from pA4 to aA8 (PS10–PS13), while *r* function is encoded by the class B and class C transcripts that accumulate from pA8 into A10 (PS14–PS15) (Boulet et al., 1991; Zavortink and Sakonju, 1989). *r* is thought to suppress *m* (Casanova et al., 1986). Epidermal *Abd-B* expression begins at the anterior margin of PS10 (Delorenzi and Bienz, 1990), while the distal limit of transcription and expression can be seen extending into PS15 (Celniker et al., 1989; Delorenzi and Bienz, 1990; Boulet et al., 1991). Since the above studies did not address the distal limits of *Abd-B* expression, one of the objectives of our study was to show that the distalmost transcription, expression and function for *Abd-B* encompass most of the tiny A10 segment.

Contributing also to the development of the posterior abdomen are *spält* (*sal*), *fork head* (*fkh*) and *caudal* (*cad*), which have homeotic phenotypes (Jürgens and Weigel, 1988). *sal* and *fkh* mutant embryos have their terminal abdominal region transformed to structures with more anterior abdominal character, suggesting that *sal* and *fkh* function independently of the BX-C genes to promote terminal development from a parasegmental ground state (Jürgens and Weigel, 1988). *fkh* mutants also broaden the most posterior *fushi tarazu* (*ftz*) stripe (Casanova, 1990), indicating that *fkh* has an additional earlier function. *cad* also has an early function that precedes metamerization of the embryo, since it has both a zygotic function that is required for the posterior terminalia and a maternal contribution that has a graded distribution (Macdonald and Struhl, 1986).

To sort out the roles of the many genes involved in the development of the tail segments, it is essential to be able to establish both the precise realm of action and exact domain of expression for each gene. Unfortunately, the paucity of identified cuticular markers in the tail region of the *Drosophila* embryo, as well as complex morphogenetic movements have hampered previous attempts. In the work described here, we have used several different molecular probes in wild-type and homeotic mutant embryos to further document the organization of the *Drosophila* tail region. This has enabled a more direct comparison between homologous structures on the embryo and larval cuticle.

2. Results

2.1. Abd-B expression extends through aA10

In order to provide epidermal landmarks for accurate assessment of mutant phenotypes and expression patterns of relevant genes, we first documented the expression patterns of *en* and *cut* in the embryonic tail. Depicted in the drawing in Fig. 1A and shown in Fig. 2A are the regions with *en* expression in the tail of stage 15 embryos. In a wild-type stage 15 embryo, stripes of epidermal cells with engrailed protein (EN) encircle the embryonic abdominal segments from pA1 to pA7, but in pA8, gaps occur between groups of epidermal cells stained with anti-engrailed antibody. Noteworthy features of the pattern of cells that contain EN in the tail region are: (1) pA8, which has a gap between the dorsal and lateral extensions, plus a small ventral component; (2) the dorsalized pA9 band which has no ventral component; (3) the hindgut; and (4) sets of neuromeres in the ventral nervous system (VNS), stained through pA9. In stage 15 embryos, no EN-containing cells were present in the lobe that separates pA9 from the anal pads, a region that is presumably A10.

Although our previous studies established the segmental identities of these regions in 3rd instar larvae (Kuhn et al., 1992) and had correlated these regions with the domains of *en* expression on the larval cuticle, we were not able to unequivocally identify the sense organs in the embryo. Since there are few other distinguishing features in the tail region, our ability to assess embryonic phenotypes in the tail has been poor. To overcome this limitation, we stained embryos with an antibody directed against the CUT protein. *cut* is expressed in all cells of each external sense organ (Blochlinger et al., 1990), and by comparing the distribution of EN and CUT in the tail of embryos and larvae, we propose that the embryonic sense organs are located as shown in Figs. 1A and 2B. All of the sense organs are in regions that do not express *en*, and are in anterior compartments.

2.2. Abd-B function extends through aA10

To correlate the domain of *Abd-B* expression with identified landmarks in the tail, the distribution of *Abd-B* RNA in stage 14 embryos was determined by *in situ* hybridization with a probe that detects both *m* and *r* transcripts. *Abd-B* RNA was prominent in the tail and abutted

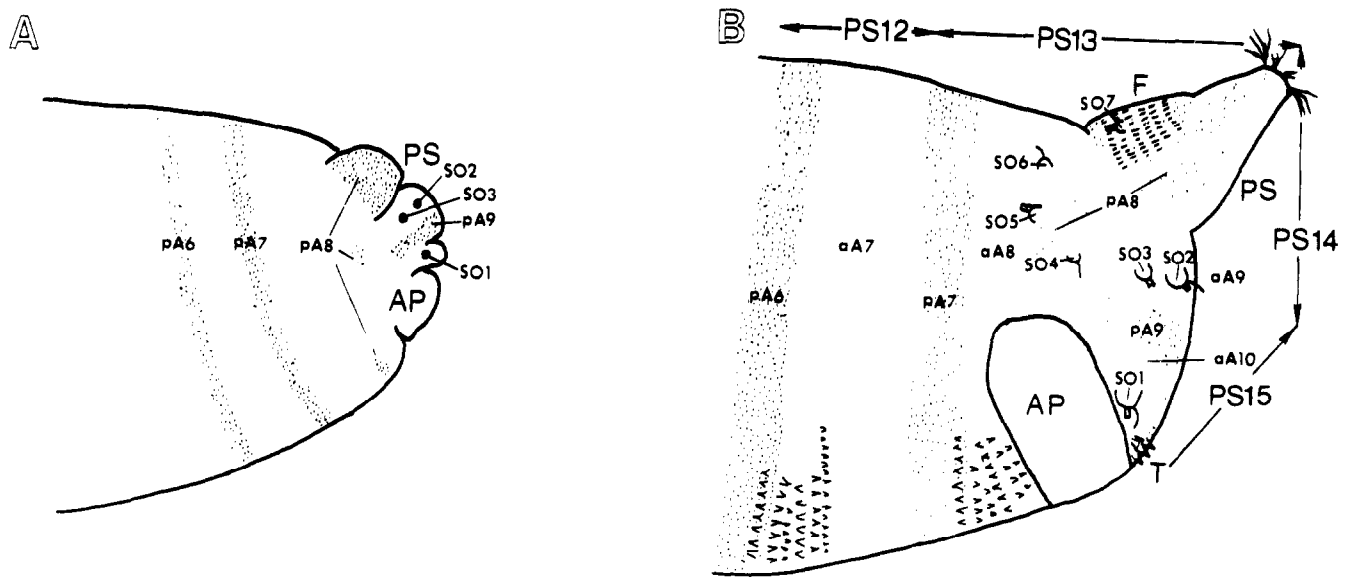

Fig. 1. Cuticular features and distribution of engrailed protein in a stage 15 embryo and a 1st instar lava. The positions of the sense organs SO1–SO3 and of engrailed-containing cells in the embryo (A) were determined after appropriate antibody staining. The distribution of engrailed-containing cells and of the sense organs in the larva (B) were as described previously for the 3rd instar larva (Kuhn et al., 1992). AP, anal pad; aA7–aA10, anterior abdominal segment 7–10; F, Fell organ; PS, posterior spiracles; PS12–PS15, parasegment 12–15; pA6–pA9, posterior abdominal segment 6–9; SO1-SO7 sense organ 1–7; T, tuft.

the anal pads (Fig. 2C). ABD-B protein in stage 15 embryos was revealed with anti-*Abd-B* antisera and was found to clearly extend through A10, which lies between the arrow and the anal pads (Fig. 2D). The anal pads do not express ABD-B protein. ABD-B protein encircles the anal pads and was present in the small aA10 region (posterior to the arrow in Fig. 2D) where SO1 is located. We conclude that BX-C function includes at its distal limits the larval SO1 in aA10 and possibly the presumptive anal tuft region which is located between the SO1s (Fig. 1A,B). At least part of the anal tuft is influenced by *Abd-B* since in BX-C$^-$ larvae, the tuft is duplicated (not pictured).

Embryonic transformations caused by *Abd-B* m^-r^+, m^+r^-, $m^{-(+)}r^{-(+)}$ and m^-r^- mutants were evaluated by analyzing the distribution of EN and by analyzing embryo morphology (Fig. 3). *M3* and *D14* are m^-r^+ *Abd-B* mutants that lack all *m* function, but retain *r* function (Kuhn et al., 1993). Adult *M3* females have eight abdominal segments, lack genitalia and (occasionally) analia, while males have eight abdominal segments and retain genitalia and analia (data not shown). In these flies, PS13 was transformed towards PS10, while PS14 was not affected. *M3* stage 14 embryos lacked posterior spiracles that derive principally from aA8 of PS13 (Figs. 3B and 5B). In these mutants, the PS14 pA8 *en* band dorsalizes, leaving a lateral gap, as in wild-type (Figs. 1A, 3A and 5A). Since there are no posterior spiracles in these embryos, the pA8 cells apparently cannot encircle, and they remain thick and straight, and retain a robust staining that is more characteristic of pA9 than of the more anterior bands. pA9 was not affected in the mutant. Similar phenotypes were noted for the m^-r^+ *D14* mutant (not shown, Fig. 5B) and for the $m^{-(+)}r^{-(+)}$ mutant *S11/S11* (Fig. 3C). The reduced *r* function of *S11* was not reflected in the shape of the pA9 band nor in the epidermal staining of ventral pA8.

Two m^+r^- mutants were examined to evaluate the effect of reduction or elimination of *r* function on the EN pattern. Both *Uab*^{1}/*Uab*^{1} and *FMA3* y^2; *tuh-3/tuh-3* flies had normal abdominal segments but males and females lacked genitalia and analia (Kuhn et al., 1993). Their most profound effect was in PS14. The stage 13 homozygous *Uab*^{1} embryo (Fig. 3D) has a pA8 EN band that was uncharacteristically straight and extended without interruption from the ventral to the dorsal surfaces (Fig. 5C). The pA9 EN band remained wild-type in that it lacked lateral and ventral extension, although a subtle lateral expansion may be present (Figs. 3D and 5C). The same results were found in *FMA3,* y^2; *tuh-3/tuh-3* embryos (not shown).

The *48* mutant is $m^{-(+)}r^-$ and is quite unusual (Kuhn et al., 1993). *48* 3rd instar larvae have a large naked cuticle region posterior to the 8th denticle band and a rather complete 9th denticle belt, suggesting that most *m* function had been lost (Kuhn et al., 1992). Stage 16 *48* embryos lacked posterior spiracles and have a pA8 EN band that fully extends from the ventral to the dorsal surface (Fig. 3E). The pA9 band was dorsal with a few EN-containing cells extending laterally.

The *Abd-B* mutants *S7*, *S4* and *D16* die as late embryos or early 1st instar larvae and lack *m* and *r* function (Kuhn et al., 1993). They all have similar effects on tail

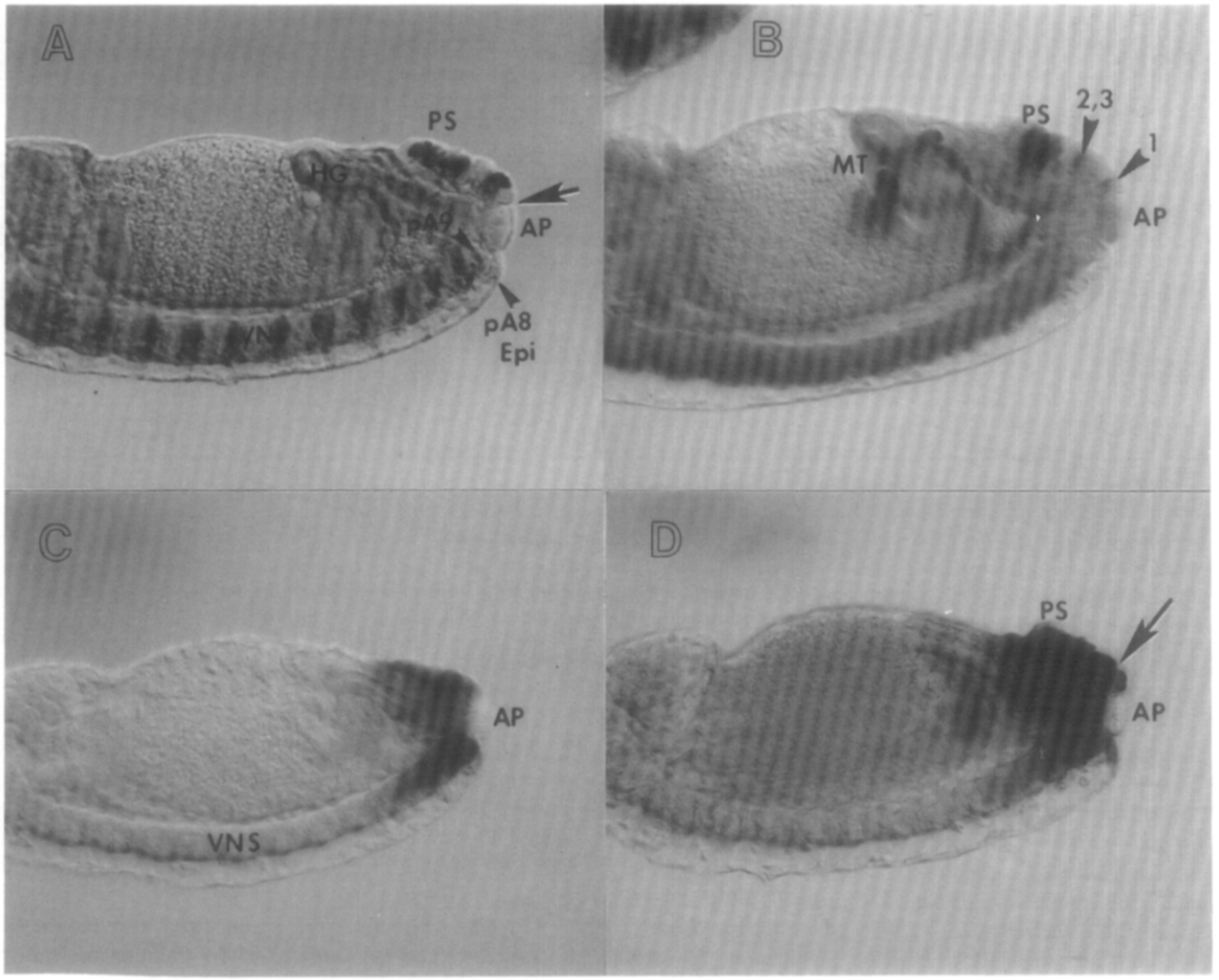

Fig. 2. Domains of *en*, *Abd-B* and *cut* expression in the embryonic tail. Stages of embryonic development follow those of Campos-Ortega and Hartenstein (1985). (A) Canton-S stage 15 embryo stained with anti-engrailed antibody. The arrow indicates where aA10 and the anal pads abut. (B) Canton-S stage 15 *cut* stained embryo. The posterior spiracles (PS) stain along with the miphigian tubules (MT). Arrowheads show positions of *cut* stained sense organs 2,3 in aA9 and 1 in aA10, which flank pA9 as seen in (A). The anal pads lack stain. (C) Canton-S stage 14 embryo in situ hybridized with the *Abd-B* common probe. Stain extends to the anal pads. (D) Stage 15 *Abd-B* stained embryo. Abd-B stain extends to the anal pads. Arrow shows position of the small dorsal *Abd-B* stained aA10. We follow the sense organ nomenclature provided in Kuhn et al. (1992) rather than that of Jürgens (1987) where SO1 is referred to as the anal sense organ. AP, anal pad; HG, hindgut MT, malphigian tubules; pA8–pA9, posterior abdominal segments 8 and 9; PS, posterior spiracles; 1–3, sense organs 1–3.

Fig. 3. Distribution of EN protein in wild-type and BX-C mutant embryos. (A) A wild-type stage 15 embryo stained with MAb 4D9 ant-EN antibody. Not visible in this embryo is the small lateral pA8 band that is depicted in Fig. 1A. (B) A stage 14 *M3* $m^{-}r^{+}$ homozygote showing a pA8 EN protein band that has dorsalized as in wild-type but in the absence of any PS, has not formed a circle. Similar effects were observed in *D14* mutant embryos. Like *M3*, *D14* retains *r* function but lacks *m* function (Kuhn et al., 1993). (C) *S11* $m^{-(+)}r^{-(+)}$ stage 13 embryo showing a straight pA8 band of cells, lacking lateral staining except for a small pA8 band. (D) A stage 13 homozygous Uab^{1} $m^{+}r^{-}$ embryo showing an uninterrupted pA8 band extending from ventral to dorsal and a slight lateral extension of pA9. (E) A stage 16 *48* homozygous $m^{-(+)}r^{-}$ embryo showing a complete pA8 band ventral to dorsal with no vestige of PS and a dorsalized pA9 band with some lateral extension. (F) A stage 14 homozygous $m^{-}r^{-}$ *S7* embryo showing a completely transformed pA8 *en* stripe encircling the embryo, with an extended pA9 band. pA8 and pA9 stain more intensely than other *en* bands and pA9 shows some limited ventral epidermal *en* staining. (G) A stage 14 *S4* homozygous $m^{-}r^{-}$ embryo showing features similar to *S7* with an expanded lateral pA9. (H) A stage 14 homozygous *Df-RK7 Abd-B*$^{-}$ embryo showing a narrow pA8 band and prominent dorsalized pA9 band. (I) The stage 15 embryo homozygous *Df-P9* BX-C^{-} embryo shows a transformation of pT2-pA7 back to pT1 as noted by the gap in lateral *en* staining. The PS do not form. (J) The *Df-P9* homozygous embryo shows that pA9 *en* stained cells retain their normal function of migrating to the dorsal side and retain their characteristic dark stain. (K) This dorsal optical view of a *Df-P9* homozygote shows a darkly stained *en* pA9 that appears to be part of a dorsal/lateral A9 component. The shape of A8 is like the segments preceding it, while the arrow identifies the junction between the small A10 and the anal pads. AP, anal pads; AS, anterior spiracles; HG, hindgut; pA8–pA9, posterior abdominal segment 8 and 9; PS, posterior spiracles; VNS, ventral nervous system.

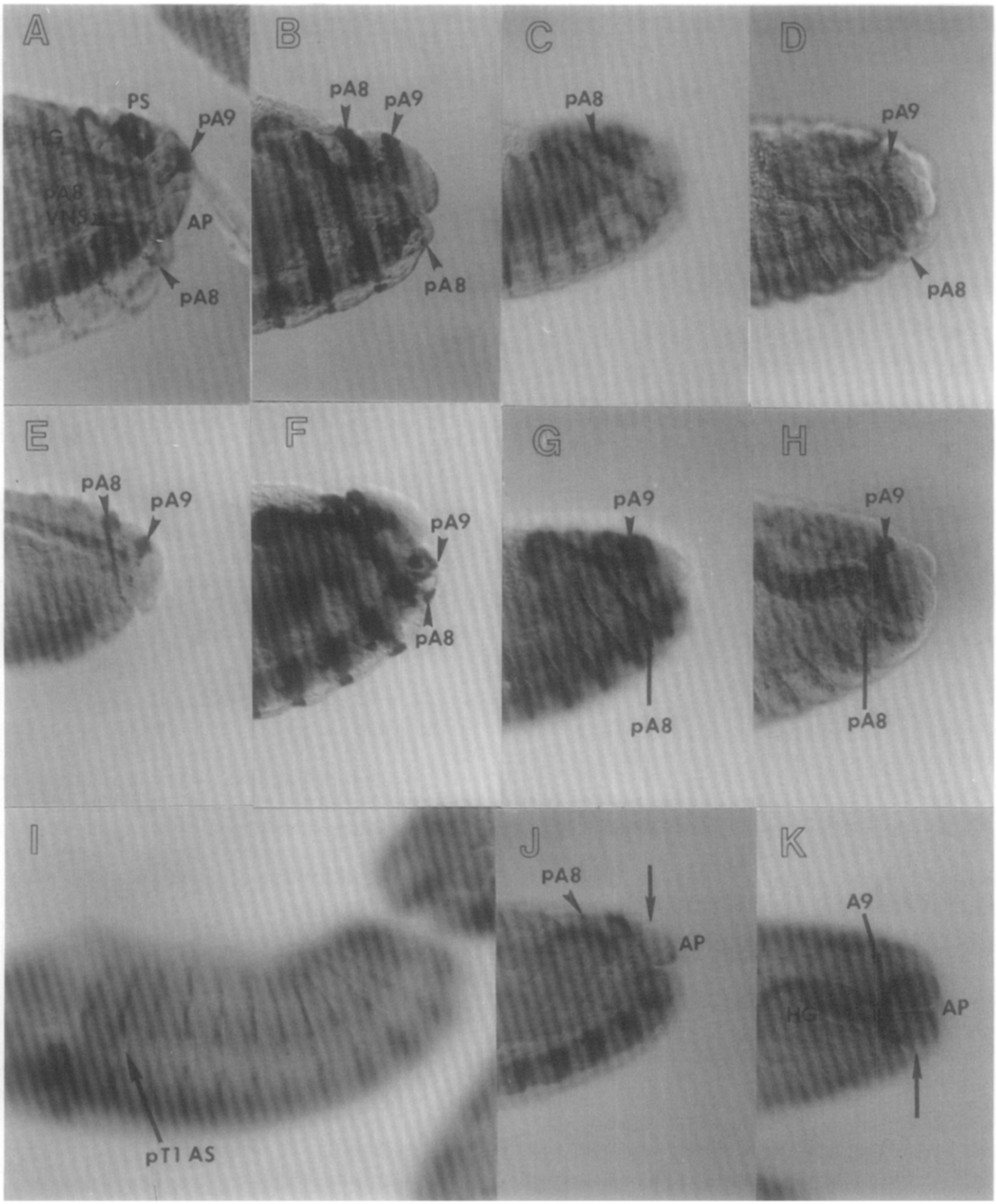

development (see drawing in Fig. 5D). The pA8 EN band of *S7* stage 14 embryos was transformed towards a more anterior character encircling the embryo in an uninterrupted manner (Figs. 3F and 5D). In aA8, no posterior spiracles formed, and a single EN-containing cell that is normally present in aA1 through aA7 was found on the lateral surface of aA8 (drawn in Fig. 5D). The pA9 band retained its basic pattern, with some lateral extension and a small ventral presence, although both the pA8 and pA9 bands were more intense than normal. EN protein in the

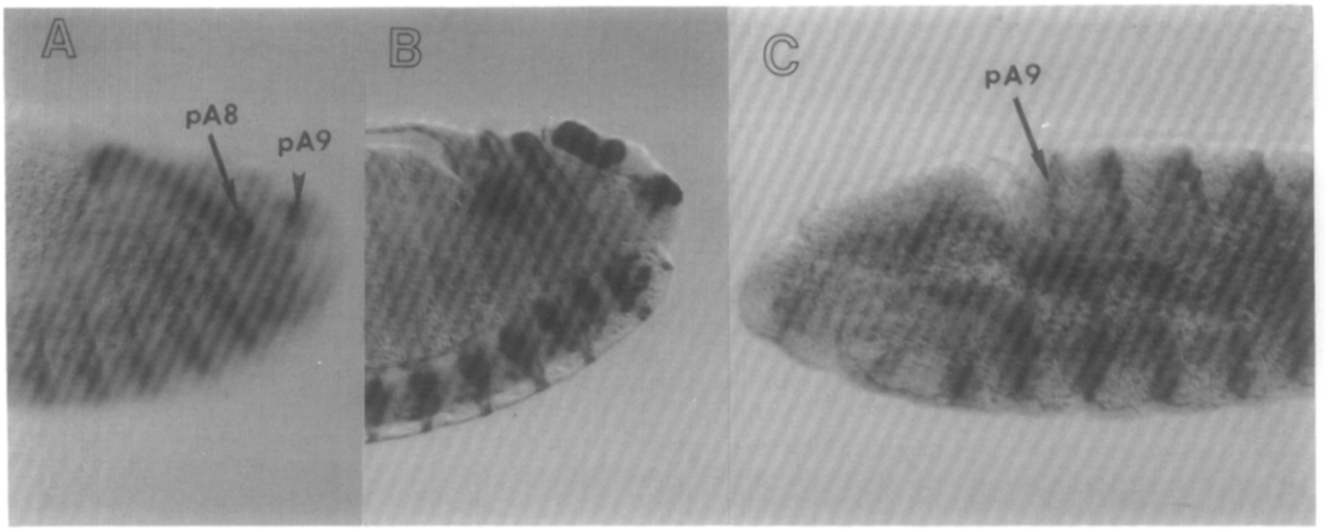

Fig. 4. Distribution of EN in sal^{2a}, cad^{2} and fkh^{XT6} mutants. (A) A stage 14 sal^{2a} embryo with reduced staining in pA8 and pA9. (B) This stage 15 fkh^{XT6} embryo has a wild-type pattern of EN in pA8 and pA9 and lacks hindgut and the anal pads. (C) This stage 12 cad^{2} embryo stained for both EN and CAD proteins has a wild-type EN pattern in pA8 and a lighter stained band in pA9.

hindgut appeared not to have been affected by lack of *Abd-B* function. The *S4* stage 14 embryo pictured in Fig. 3G was similar to *S7*, with its pA8 band extending completely around the embryo. Its pA9 band was extended more laterally. The EN patterns in *D16* embryos (not shown) were basically the same as *S7* and *S4*. The general epidermal staining pattern for $m^{-}r^{-}$ mutants is shown in Fig. 5D.

Df-RK7 is a deletion that removes the entire *Abd-B* coding region (Duncan, pers. commun.). Stage 14 *Df-RK7* embryos had a narrow pA8 EN band reflecting the pA8 transformation towards pA4 (Figs. 3H and 5E). The pA9 EN lateral bands fused dorsally and were more prominent than the other abdominal bands in thickness and intensity.

Patterns of EN protein in embryos deficient for the entire BX-C (*Df-P9*) are shown in Figs. 3I, 3J and 3K, summarized in Fig. 5F. Absence of BX-C function results in transformation of thoracic and abdominal segments to pT1/aT2 (PS4). This transformation is manifested in the shape of the EN bands, which in normal embryos are continuous except in pT1. In pT1, a gap in the band is left where the anterior spiracles form. In *Df-P9* embryos, the EN stripes from pT1 to at least pA7 all had a lateral gap in the same location (Figs. 3I and 5F). In addition, the posterior spiracles which principally derive from aA8 were absent because this region is also transformed towards thorax. In pA8, a thin band of EN-containing cells, with no obvious gap, appeared as normally found on more anterior segments (Figs. 3J and 5F). Unfortunately for reasons that are not clear, staining was always light, making it difficult to visualize pA8. Unexpectedly, the pA9 band remained as intense as in the wild-type embryos, although pA9 VNS staining was reduced. The dorsal view in Fig. 3K clearly shows the dark pA9 dorsal band and the stained hindgut. The shape of A9 appears to show a lateral/dorsal component only, while distal to pA9 the region is clearly separated (see arrow) into aA10 and anal pads. Because of the EN bands and embryo morphology we conclude that the role of the BX-C as the primary purveyor of segmental identity extends through A8, but that the more posterior regions require additional input from other genes.

2.3. Effect of sal, cad, and fkh on EN patterns

The non-BX-C mutants with homeotic phenotypes sal^{2a}, cad^{2} and fkh^{XT6} have been shown to affect the identity of posterior segments (Jürgens, 1987, 1988; Jürgens and Weigel, 1988; Macdonald and Struhl, 1986). To map their effects more precisely, patterns of EN were documented in mutant embryos. The sal^{2a} stage 14 embryo in Fig. 4A has defects in pA8 and pA9. The pA8 EN-containing cells that should encircle the posterior spiracles are confined to an irregular and reduced cluster of cells localized to the posterior side of the spiracular region (Fig. 4A, Fig. 5G). The majority of the sal^{2a} homozygous embryos do not form distinct posterior spiracles (data not shown). pA9 staining in these mutants was variable and was frequently reduced (Fig. 5G). We can distinguish the sal^{2a} homozygotes from their sibs because sal^{2a} is balanced with a second chromosome carrying a *Ubx*-lacZ insert. Thus, embryos lacking the *Ubx* pattern are homozygous for the mutant gene. These embryos retained EN in the hindgut. In fkh^{XT6} mutants where anal pads and hindgut are missing in both larvae (Jürgens, 1987) and embryos (Fig. 4B), the EN bands in pA8 and pA9 were wild-type (Figs. 4B and 5H). EN patterns in stage 12 cad^{2} *en*-cad^{2} double stained mutant embryos were essentially normal in pA8 and pA9 (Figs. 4C and 5I). However by stage 15, cad^{2} embryos lacked a complete pA9 EN band in the double stained embryos (not

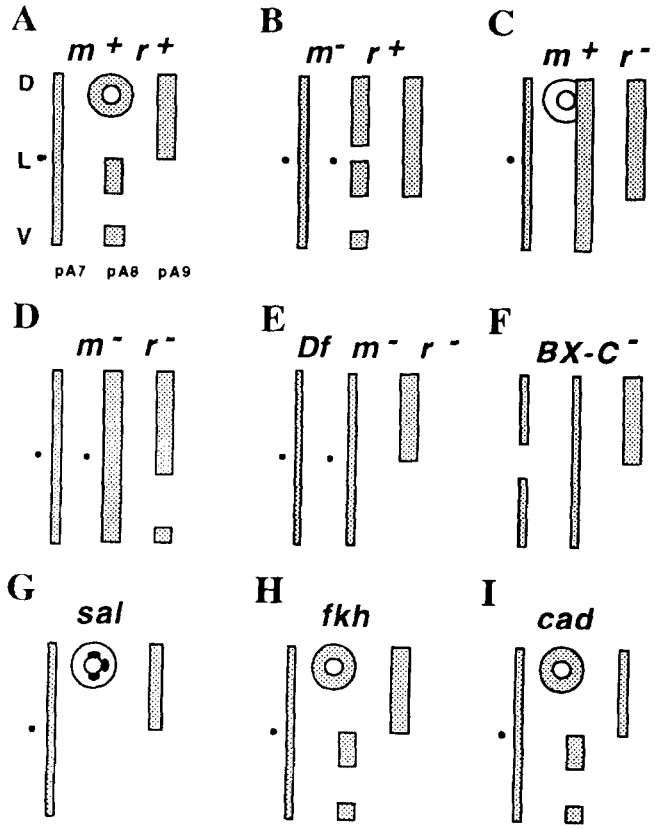

Fig. 5. Schematic presentation of embryonic epidermal *en* expression in pA7–pA9 for BX-C mutants and for mutants with homeotic phenotypes. The *en* pattern alterations caused by the BX-C mutants and by the other mutants with homeotic phenotypes were not always obvious in the tail segments because the photographs reflect one focal plane. Figs. 3 and 4 picture embryos, while Fig. 5 summarizes relevant *en* patterns from pA7 to pA9. Circles represent posterior spiracles with *en* cells within. Bands and partial bands show expression patterns from dorsal to ventral. (A) m^+r^+ wild-type *en* pattern with complete band in pA7, interrupted band in pA8 and dorsal-lateral band in pA9. (B) m^-r^+ *en* pattern for *M3* and *D14* shows lack of posterior spiracles and straight pA8 band with gaps. (C) m^+r^- *en* patterns for Uab^1 and *tuh-3* show the uninterrupted pA8 band. (D) m^-r^- *en* pattern for the *S4*, *S7* and *D16* mutants showing uninterrupted pA8 band with the single aA8 *en* cell and the lengthened pA9 lateral band with some *en* expression ventrally in pA9. (E) m^-r^- *Abd-B*$^-$ *en* pattern for *Df-RK7* with complete pA8 band. (F) BX-C$^-$ *en* pattern of *Df-P9* homozygotes showing interruption in pA7 band, uninterrupted pA8 band and dorsal-lateral pA9 band. (G) sal^{2a} *en* pattern with reduced pA8 and pA9 *en* expression. (H) fkh^{XT6} *en* pattern which is normal for pA7–pA9. (I) cad^{2a} pattern showing reduced pA9 *en* expression. D, dorsal; L, lateral; V, ventral.

shown). This result is consistent with the report that cad^2 affects much of pA9 and aA10 (PS15) (Macdonald and Struhl, 1986).

2.4. Expression of cad, Abd-B and en in pA9 and aA10

Expression of *cad*, *Abd-B*, and *en* in pA9 and aA10 (PS15) reflects the actively changing nature of this region. In stage 12 germband extended embryos, *cad* distribution appeared limited to aA10 of PS15, and surrounds much of the presumptive anal pads (Fig. 6A). The CAD-containing cells do not appear to contain EN and there is little evidence of *cad* expression on the posterior side of the presumptive anal pad in the double stained embryo (Fig. 6A). Slightly later in stage 12, there was a distinct band of CAD-containing cells that complete the circle around the posterior side of the anal pads (Fig. 6B). As germband retraction continues, the pA9 EN-containing cells and CAD containing cells progressively dorsalize (Fig. 6C), and some cells appeared to contain both CAD and EN. Next, two pads of CAD expressing cells appear posterior to the anal pads (Fig. 6D). The late stage 12 embryo in Fig. 6E shows two large groups of CAD-containing cells with their outer rim of EN-containing cells, which have essentially completed dorsalization. At stage 16, CAD-containing cells resolve to two lines of cells encircling the anal pads, one outside the anal pad border and the other just inside the anal pads (Fig. 6F). These patterns share some features with the domains of Abd-B-containing cells, which overlap on the ventral and lateral sides in stage 12 embryos and dorsalize to surround the anal pads in later stages (Fig. 6G,H). Comparisons between Fig. 6B,C and Fig. 6G clearly show that *Abd-B* is not expressed posterior to the anal pads where CAD-containing cells stain. These data show that *Abd-B* function may not include all of the *cad* domain. The stage 15 embryo in Fig. 6I shows that a pA9 band of EN-containing cells projects from the midpoint of the fused pA9 band distally toward the anal pads. This projection occurs after dorsally migrating pA9 bands on each side of the embryo fuse. It is the last element of the EN pattern to develop. This perpendicular extension of the EN cells terminates beneath the larval anal tuft (see drawing in Fig. 1B).

3. Discussion

3.1. Identifying tail segments

This analysis of the embryonic tail as well as previous studies of 1st (Jürgens, 1987) and 3rd instar larvae (Kuhn et al., 1992), demonstrate that the tail segments are highly modified and predominantly comprised of lateral and dorsal tissue. Progenitor cells for ventral regions between the 8th denticle belt and aA10 are not present after germband retraction. In addition to the apparent deletion of these ventral regions, dorsal migration during the final stages of germband retraction and further movements during later embryonic stages rearranges the progenitor cells of the tail. As a consequence, establishing the segmental origins of the tail has been problematic. We focus here on the organization of the tail, using patterns of expression of several segmentation and homeotic genes in both wild-type and mutant embryos to infer both the history and relationships of various tail structures.

The identity and origins of pA8, aA9 and pA9 were determined by documenting the history of EN-containing cells. Adjacent and posterior to pA9 in the 1st instar larva is cuticle with SO1s, the anal tuft and the anal pads. The

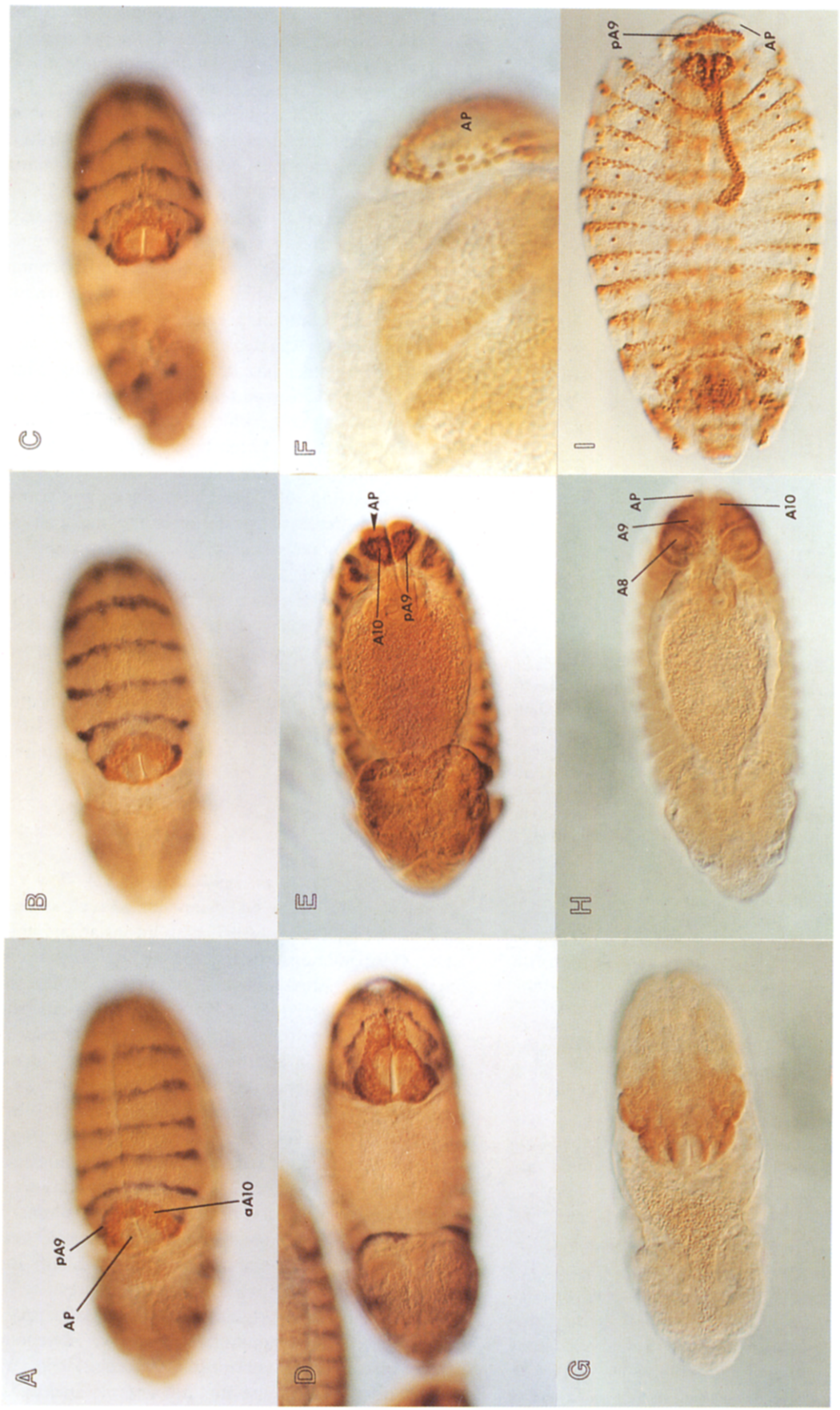

Fig. 6. Expression of *cad*, *Abd-B*, and *en* in PS15. (A–F) Dorsal views of *ryXho25* embryos with brown (CAD) and blue (β-galactosidase) staining indicating the regions with CAD and EN expression, respectively. (A–D) Stage 12 embryos. In (A), CAD-containing cells surround all but the posterior side of the anal pads. Note the smooth appearance of the blue staining that is characteristic of cytoplasmic localization and the granular appearance of the nuclear-localized brown stain. (B) A later stage 12 embryo with CAD-expressing cells encircling the anal pads. (C,D) Stage 12 embryos with pA9 cells dorsalizing. (E) The cells containing CAD posterior to the anal pads continues to expand during stage 13. (F) A stage 16 embryo with a band of CAD-containing cells that overlaps the anal pad border. (G) During germband retraction, ABD-B protein is present in a region that surrounds all but the most posterior aspect of the anal pads. (H) ABD-B protein in this stage 14 embryo encircles the anal pads in the aA10 region. (I) Extension of the pA9 EN band toward the anal pads in a stage 15 embryo.

SO1s, the anal tuft, and the cuticle posterior to the A8 denticle belt are abnormal in *Abd-B* mutant larvae, and in stage 14–15 embryos the SO1 anlage is in a region in which *Abd-B* is expressed. Since the genes of the BX-C are expressed in a parasegmental manner, and since *Abd-B* expression and function extends beyond pA9, we conclude that cuticle distal to pA9, probably including the anal tuft, are partially controlled by *Abd-B* and are primarily produced by aA10. Supporting this conjecture are the observations that the most posterior stripe of *FTZ* expressing cells extends beyond pA9, coincides with the distribution pattern of the *Abd-B* class-B transcript (data not shown), and the number of tuft denticles is reduced to about two in *ftz* mutant embryos (Jürgens, 1987).

The origin of the anal tuft is problematic. In 1st and 3rd instar larvae (Kuhn et al., 1992), a band of EN-containing cells extends from pA9 between the SO1s to the denticles of the anal tuft and the anal pad (Fig. 1B). This band forms during stage 15 (Fig. 6I), apparently by budding from pA9 as the pA9 bands dorsalize. Since some cells beneath the tuft stain with anti-EN antibody and since the number of tuft denticles is reduced from an average of 12 to 8 in *en* mutants (Jürgens, 1987), it appears that the anal tuft is partially of posterior compartment origin. In light of the oblique movements of the pA9 cells, it is conceivable that the posterior tuft-producing cells are of pA9 origin, with the remainder from aA10. However, it is also possible that the EN-containing cells beneath the tuft denticles are from a tiny pA10. The extended pA9 and proposed pA10 could become juxtaposed during embryogenesis when pA9 dorsalizes (see Fig. 6), leaving the A10 CAD-containing cells between them and the anal pads. This would put pA9 cells next to pA10 cells if they exist. The difficulty of the tuft denticles deriving from cells extending from the pA9 band is that tuft denticles are presumably ventral structures, whereas the extended *en* band comes from the dorsal-most pA9 cells. It would seem unlikely that these cells would secrete ventral denticles.

3.2. *en* embryonic patterns reveal BX-C functions

en staining patterns in *Df-P9* embryos revealed a transformation of the entire embryo between PS5 (pT2–aT3) and PS14 (pA8–aA9) to PS4 (pT1–aT2) (see review by Duncan, 1987). The spiracles that form in pT1 create a gap in the *en* stripe, and whereas the *en* stripes of wild-type embryos have the spiracular gap in only pT1, ten of the stripes of *Df-P9* embryos (pT1–pA7) were gapped. Importantly, although pA8 was mostly transformed, it did not have an obvious gap, and pA9 did not significantly deviate from wild-type. We interpret these observations to mean that the BX-C alone provides segmental identity to PS5 to PS13, but other genes in addition to the BX-C affect the level of development of PS14 and PS15. This is in agreement with Jürgens (1988), who interpreted the phenotype of BX-C$^-$ embryos as PS5 to PS12 transformed to PS4, PS13 changed to a modified PS4, and PS14 and PS15 transformed to a hybrid between head and thorax.

en patterns in *Abd-B* mutants reveal how the *m* and *r* functions affect different parts of the tail. In m^-r^+ mutants, no posterior spiracles form and pA8 does not surround the spiracles as it normally would. Instead, pA8 remains straight and the gap in lateral staining is retained. pA8 also remains straight in m^+r^- embryos and has a shape similar to the posterior stripes of the more anterior abdominal segments, showing that the gap requires *r* function. pA9 is not markedly changed in these embryos, although both the transformed *en* bands in pA8 and the band in pA9 are more intensely stained than *en* bands in more anterior abdominal segments. Complete transformation of both pA8 and pA9, to more anterior character yield pA8 and pA9 bands that extend completely around the ventral surface in some m^-r^- embryos. Thus, one function of *m* and *r* apparently involves suppression of ventral structures in pA8 and A9. Curiously, m^-r^- larvae did not differentiate ventral A9 epidermal structures. We do not know whether ventral A9 cells do not secrete cuticle, suffer apoptosis, or whether they contribute to internal rather than epidermal tissues. Due to the ambiguous and inconclusive nature of the putative pA10 *en* cells, we could not evaluate possible transformations of pA10 in BX-C mutants.

3.3. Non-BX-C homeotic genes influence the identity of the tail segments

In addition to *Abd-B*, the *empty spiracles* (*ems*) gene is required for normal development of the larval Filzkörper and is transcriptionally regulated by *Abd-B* (Jones and McGinnis, 1993). A third gene required in A8 is *sal*, mutants of which cause transformations in terminal segments (Jürgens, 1988; Kühnlein et al., 1994). Disorganization occurs in A8, while A9 and A10 incompletely transform toward A8. Lack of *sal* function results in transformations confined to lateral and dorsal structures (Kuhn, unpublished). However, *sal*; *Abd-B* double mutants have a complete thoracic A9 segment and a rudimentary dorsal A10 that has been transformed to thorax as well (see Jürgens, 1988). The addition of the transformed ventral A9 in the double mutant suggests that *Abd-B*, not *sal*, suppresses ventral structures. A different gene is envisioned to suppress ventral A10, since this pattern element was not added back in the double mutant. One candidate for such a gene could be *cad*, a homeotic gene with both maternal and zygotic functions (Macdonald and Struhl, 1986; Mlodzik and Gehring, 1987). *cad* mutants lacking zygotic function are deficient for SO1, the tuft and portions of the anal pads (Macdonald and Struhl, 1986). When the *cad* maternal component was also missing, then deletions were observed in even numbered segments with most of A8 and A10 deleted and replaced by small sclerotized tissue resembling mouth hooks (Macdonald and

Struhl, 1986). The presence of sclerotized tissue in the tail region of *cad* mutant larvae can be interpreted to mean that *cad* is required for *Abd-B* function. Sclerotized plates appear in the *Df-P9* tail, forming on the ventral surface. In *cad* mutant larvae, plates are expressed between A7 and the modified anal pads. These larvae were quite deformed (see Macdonald and Struhl, 1986), so it is difficult to know if the pA9–aA10 region has acquired a ventral component. However, since the pA9 EN band does not extend around the ventral surface in zygotic loss of function *cad* embryos (Fig. 3B), then either maternal expression of *cad* is sufficient for ventral suppression, or ventral suppression is a function of a yet to be identified gene.

4. Materials and methods

4.1. Drosophila stocks

(1) Canton-S is an m^+r^+ wild-type laboratory strain. (2) *ryXho25* is a strain in which the *E. coli* lacZ gene is expressed under the control of the *engrailed* promoter (Hama et al., 1990). (3 and 4) *S7* and *S4* are BX-C *Abd-B* m^-r^- mutants (Tiong et al., 1988). (5) *Df-RK7* is a BX-C *Abd-B* m^-r^- deficiency, Df(89E-90) (Duncan, pers. commun.). (6) D16 is a BX-C *Abd-B* m^-r^- mutation (Boulet et al., 1991) (7) M3 is a BX-C *Abd-B* m^-r^+ mutation (Sánchez-Herrero, 1991). (8) *D14* is a BX-C *Abd-B* m^-r^+ mutant (Karch et al., 1985). (9) *S11* is a BX-C *Abd-B* $m^{-(+)}r^{-(+)}$ spontaneous mutation reducing both *m* and *r* function (Kuhn et al., 1993; Tiong et al., 1988). (10) *48* is a BX-C *Abd-B*$^{-(+)}r^-$ mutation in In(89E-100C) that shows reduced *m* function (Kuhn et al., 1993). (11) *65* is a BX-C *Abd-B* m^+r^- mutation associated with T(2;3)89E/41 (Karch et al., 1985). (12) *Uab*^{1} is a BX-C *Abd-B* m^+r^- mutation associated with a tiny BX-C inversion (Karch et al., 1985). (13) *tuh-3* is a BX-C *Abd-B* m^+r^- spontaneous mutation (Karch et al., 1985; Kuhn et al., 1993). (14) *fkh*^{XT6} is a mutation affecting embryonic larval terminal regions (Jürgens and Weigel, 1988; Lindsley and Zimm, 1992). (15) *sal*^{2a} is also a mutation causing homeotic transformations to terminal structures (Jürgens, 1988; Lindsley and Zimm, 1992). (16) *cad*^{2} is a maternal and zygotic homeobox mutant affecting distal structures (Macdonald and Struhl, 1986; Lindsley and Zimm, 1992).

4.2. Stock maintenance

All *Drosophila* stocks were maintained at room temperature, approximately 24°C, on a standard medium consisting of cornmeal, agar, dextrose, sucrose, dried yeast extract, propionic acid and phosphoric acid. Tegosept was added to the surface of the dried medium just prior to use to further suppress mold growth.

4.3. Antibody staining of embryos

EN (engrailed) protein was detected with MAb 4D9, which detects both EN and INV (invected) proteins (Patel et al., 1989). We assume here that all cells stained by 4D9 belong exclusively to the posterior compartment of each segment and that unstained cells are located in anterior compartments. Details of the staining procedure are provided in Karr et al. (1989) and Patel et al. (1989). The general procedure for MAb 4D9 antibody staining of whole mount embryos was also used for the other antibodies employed in this study, except where noted.

β-Galactosidase protein was detected by incubation in a 1:1000 dilution of a rabbit anti-β-galactosidase IgG for 45 min. Incubation was with alkaline phosphatase-coupled secondary goat antibody diluted 1:500. Final washes were in a high pH buffer (100 mM NaCl, 50 mM $MgCl_2$, 100 mM Tris (pH 9.5), 0.1% Tween-20). The color reaction was monitored in 1 ml of the high pH buffer with 4.5 μl NBT + 3.5 μl BCIP.

CAD (caudal) protein was detected in *ryXho25* embryos that were also stained for β-galactosidase protein by incubating both primary antibodies together. Rat α-anti-CAD p312 antibody was diluted in PBT 1:50 and was preadsorbed against a large volume of embryos at 4°C overnight to reduce background. Rabbit anti-β-galactosidase was used at a 1:200 dilution. After blocking, secondary antibodies were added, using as a tertiary reagent the ABC reagent from the Vectastain elite kit to enhance the peroxidase detection of CAD, followed by the alkaline phosphatase reaction to detect β-galactosidase. Biotinylated goat anti-rat IgG was used at a 1:125 dilution and alkaline phosphatase conjugated goat anti-rabbit IgG was used at a 1:200 dilution.

CT (cut) protein was detected in Canton-S embryos, with cobalt chloride and nickel sulfate added to enhance the signal. Anti-CT F2 rat polyclonal antibody was diluted 1:500 in PBT, and bovine serum albumin was included with the primary and secondary antibodies to reduce background staining.

ABD-B protein was detected with mouse MAb 1A2E9 (Celniker et al., 1989) and a peroxidase-coupled secondary antibody. In situ hybridization with the *Abd-B* common probe followed published procedures (Boulet et al., 1991; Kuhn et al., 1993). The digoxigenin-labeled probe was prepared by asymmetric PCR amplification. The common probe recognizes all *Abd-B* transcripts for *m* and *r* functions.

Acknowledgments

We sincerely thank Drs. Welcome Bender and David H. Vickers for their helpful discussions and constructive comments on this manuscript and to Dr. Haven Sweet for help with the computerized figure. We are most grateful to Drs. Bender, Celniker, Sakonju, Blochlinger, Struhl and the Indiana Stock Center for generously supplying antibodies, probes and fly strains that made this study possible. Support was provided by NSF research grants RUI DMB-9023293, MCB-9418119 to D.T.K., NIH

grants to T.B.K. and summer research fellowships to G.T. by ACS, Fla. Div. Inc.

References

Baumgartner, S., Bopp, D., Burri, M. and Noll, M. (1987) Genes Dev. 1, 1247–1267.

Blochlinger, K., Bodmer, R., Jan, L.Y. and Jan, Y. N. (1990) Genes Dev. 4, 1322–1331.

Bopp, D., Burri, M., Baumgartner, S., Frigerio, G. and Noll, M. (1986) Cell 47, 1033–1040.

Boulet, A.M., Lloyd, A. and Sakonju, S. (1991) Development 111, 393–405.

Campos-Ortega, J.A. and Hartenstein, V. (1985). The embryonic development of *Drosophila melanogaster*. Springer-Verlag, Berlin.

Casanova, J. (1990) Development 110, 621–628.

Casanova, J., Sánchez-Herrero, E. and Morata, G. (1986) Cell 47, 627–636.

Celniker, S.E., Keelan, D.J. and Lewis, E.B. (1989) Genes Dev. 3, 1424–1436.

Delorenzi, M. and Bienz, M. (1990) Development 108, 323–329.

Duncan, I. (1987) Annu. Rev. Genet. 21, 285–319.

Gutjahr, T., Patel, N.H., Li, X., Goodman, C.S. and Noll, M. (1993). Development 118, 21–31.

Hama, C., Ali, Z. and Kornberg, T.B. (1990) Genes Dev. 4, 1079–1093.

Hidalgo, A. (1991) Mech. Dev. 35, 77–87.

Jones, B. and McGinnis, W. (1993) Genes Dev. 7, 229–240.

Jürgens, G. (1987) Wilhelm Roux's Arch. Dev. Biol. 196, 141–157.

Jürgens, G. (1988). EMBO J. 7, 189–196.

Jürgens, G. and Weigel, D. (1988) Wilhelm Roux's Arch. Dev. Biol. 197, 345–354.

Jürgens, G. and Hartenstein, V. (1993) The development of *Drosophila melanogaster*. Cold Spring Harbor Press, Cold Spring Harbor, NY, pp. 687–746.

Karr, T.L., Weir, M.P., Ali, Z. and Kornberg, T. (1989) Development 105, 605–612.

Kühnlein, R.P., Frommer, G., Friedrich, M., Gonzalez-Gaitan, M., Weber, W., Gehring, W.J., Jäckle, H. and Schuh, R. (1994) EMBO J. 13, 168–179.

Karch, F., Weiffenbach, B., Peifer, M., Bender, W., Duncan, I., Celniker, S., Crosby, M. and Lewis, E.B. (1985) Cell 43, 81–96.

Kuhn, D.T., Sawyer, M., Packert, G., Turenchalk, G., Mack, J.A., Sprey, Th. E., Gustavson, E. and Kornberg, T.B. (1992) Development 116, 11–20.

Kuhn, D.T., Mack, J.A., Duan, C. and Packert, G. (1993) Genetics 133, 593–604.

Lawrence, P.A. and Morata, G. (1994) Cell 78, 181–189.

Lewis, E.B. (1978) Nature 276, 565–570.

Lindsley, D.J. and Zimm, G.G. (1992) The genome of *Drosophila melanogaster*. Academic Press, New York.

Macdonald, P.M. and Struhl, G. (1986) Nature 324, 537–545.

McGinnis, W. and Krumlauf, R. (1992) Cell 68, 283–302.

Mlodzik, M. and Gehring, W.J. (1987) Cell 48, 465–478.

Patel, N.H., Martin-Blanco, E., Coleman, K.G., Poole, S.J., Ellis, M.C., Kornberg, T.B. and Goodman, C.S. (1989) Cell 58, 955–968.

Sánchez-Herrero, E. (1991) Development 111, 437–449.

St. Johnston, R.D. and Nüsslein-Volhard, C. (1992) Cell 68, 201–219.

Tiong, S.Y.K., Gribbin, M.C. and Whittle, J.R.S. (1988) Wilhelm Roux's Arch. Dev. Biol. 197, 131–140.

Zavortink, M. and Sakonju, S. (1989) Genes Dev. 3, 1969–1981.